THE JOURNAL OF BIOLOGICAL CHEMISTRY VOL. 285, NO. 37, pp. 28627–28634, September 10, 2010

Effects of Regulator of G Protein Signaling 19 (RGS19) on Heart Development and Function*

Received for publication, October 13, 2009, and in revised form, June 11, 2010 Published, JBC Papers in Press, June 18, 2010, DOI 10.1074/jbc.M109.073718

Young Rae Ji[‡], Myoung Ok Kim[‡], Sung Hyun Kim[‡], Dong Hun Yu[‡], Mi Jung Shin[‡], Hei Jung Kim[‡], Hyung Soo Yuh[‡], Ki Beom Bae[‡], Jae Young Kim[§], Hum Dai Park[‖], Sang Gyu Lee[‡], Byung Hwa Hyun[¶1], and Zae Young Ryoo[‡1,2]

From the [‡]School of Life Science and Biotechnology, Kyungpook National University, 1370 Sankyuk-dong, Buk-ku, Daegu 702-701, Korea, the [§]Department of Biochemistry, School of Dentistry, Brain Korea 21 Project, IHBR, Kyungpook National University, Daegu, 702-701, Korea, the [¶]Disease Model Research Center, Korea Research Institute of Bioscience and Biotechnology, Daegeon 305-806, Korea, and the [‖]Department of Biotechnology, School of Engineering, Daegu University, 15 Jillyang, Gyeongsang, Gyeongbuk 712-714, Korea

Wnt/Wg genes play a critical role in the development of various organisms. For example, the Wnt/β-catenin signal promotes heart formation and cardiomyocyte differentiation in mice. Previous studies have shown that RGS19 (regulator of G protein signaling 19), which has Gα subunits with GTPase activity, inhibits the Wnt/β-catenin signal through inactivation of $G\alpha_o$. In the present study, the effects of RGS19 on mouse cardiac development were observed. In P19 teratocarcinoma cells with RGS19 overexpression, RGS19 inhibited cardiomyocyte differentiation by blocking the Wnt signal. Additionally, several genes targeted by Wnt were down-regulated. For the *in vivo* study, we generated RGS19-overexpressing transgenic (RGS19 TG) mice. In these transgenic mice, septal defects and thin-walled ventricles were observed during the embryonic phase of development, and the expression of cardiogenesis-related genes, BMP4 and Mef2C, was reduced significantly. RGS19 TG mice showed increased expression levels of brain natriuretic peptide and β-MHC, which are markers of heart failure, increase of cell proliferation, and electrocardiogram analysis shows abnormal ventricle repolarization. These data provide *in vitro* and *in vivo* evidence that RGS19 influenced cardiac development and had negative effects on heart function.

The mammalian regulator of G protein signaling (RGS)[3] family consists of >20 members (1). RGS proteins have been grouped into subfamilies (RZ, R4, R7, R12, and RA) based on sequence conservation in the RGS domain (2). RGS proteins possess GTPase functions and interact with GTP-Gα subunits to limit their lifespan and terminate downstream signaling (2, 3). RGS19, one of the first discovered RGS members, is a small protein with 216 residues (mouse). RGS19 interacts selectively with α subunits of most inhibitory G proteins ($G\alpha_i$, $G\alpha_q$) and enhances their GTPase activity (4).

Wnt/Wg genes, which are related to the wingless genes in *Drosophila*, encode a number of secreted proteins that play critical roles in the development of various organisms, via cell fate and patterning (5). During early embryogenesis, Wnt signaling is essential for primitive streak formation and mesoderm induction. Later, the Wnt signal is necessary for patterning of the anterior-posterior body plan, trunk/tail development, and specification of posterior mesodermal fates. However, Wnt inhibition is required in head formation (6, 7).

Heterotrimeric G-proteins are necessary to the Wnt/β-catenin pathway (8). $G\alpha_o$ and $G\alpha_q$ are required for Wnt-stimulated target gene activation. During the inactivation stage, the GDP-Gα subunit complexes with the Gβ-Gγ dimer. G-proteins activated by the G-protein-coupled receptor are exchanged for GTP by the Gα subunit, and dissociation of the Gβ-Gγ dimer occurs (9). Both the GTP-Gα subunits and the free Gβ-Gγ dimers activate downstream signaling molecules.

In the canonical Wnt/β-catenin pathway, cytosolic levels of β-catenin are regulated by a protein complex that includes glycogen synthase kinase 3β, Axin, and adenomatous polyposis coli (10). Within the complex, β-catenin is phosphorylated and targeted for degradation by the proteasome pathway in unstimulated cells (11). In stimulated cells, Wnt binds to the Frizzled (Fz) family receptors and activates an associated downstream component, Dishevelled, which leads to inactivation of glycogen synthase kinase 3β, thereby stabilizing β-catenin. Accumulated β-catenin in the cytosol enters the nucleus, thereby leading to the interaction with T-cell factor/lymphoid enhancer binding factor transcription factors and transcription of Wnt-responsive genes.

Presently, there is contradictory evidence regarding the role of Wnt signaling in heart formation and cardiomyocyte differentiation, depending on the model organism used. In chick and *Xenopus*, the Wnt/β-catenin signal inhibits cardiac development, because expression of Wnt inhibitors in the tissues adjacent to cardiac mesoderm is necessary for cardiogenesis (12, 13). In contrast, the Wnt/β-catenin signal promotes heart formation in *Drosophila* (14) and induces cardiomyocyte differentiation in a mouse embryonic carcinoma cell line, P19CL6 (15). Thus, Wnt/β-catenin signaling inhibits cardiogenesis in chick

* This work was supported in part by Grant NRF2009-0088343 from the National Research Foundation of Korea, SRC Program of Korea Science and Engineering Foundation (KOSEF) Grant 2009-0063409 (funded by the Korean government), and the Regional Care Research Program from the Korea Ministry of Education, Science, and Technology.

[1] Both authors contributed equally to this work.

[2] To whom correspondence should be addressed: School of Life Sciences and Biotechnology, College of Natural Sciences, Kyungpook National University 1370 Sankyuk-dong, Buk-ku, Daegu 702-701, Korea. Tel.: 82-53-950-7361; Fax: 82-53-943-6925; E-mail: jaewoong64@hanmail.net.

[3] The abbreviations used are: RGS, regulator of G protein signaling; α-MHC, α-myosin heavy chain; cTnT, cardiac troponin T; TG, transgenic.

TABLE 1
PCR primers used in RT-PCR

Gene	Primer sequence	Amplicon size
Brachyury T (NM_009309)	Forward, 5′-tctgacagccagtatgacac-3′; reverse, 5′-atataggaccctacctagca-3′	378 bp
Wnt3a (NM_009522)	Forward, 5′-ggcaaggcttcactgaagac-3′; reverse, 5′-aggcaacatctctgaggcat-3′	531 bp
GATA4 (NM_008092)	Forward, 5′-tcctgaagaacaactgggta-3′; reverse, 5′-aagtagacaccctgctcaga-3′	329 bp
Pax3 (NM_008781)	Forward, 5′-acctcagtcagatgaaggct-3′; reverse, 5′-agtcccattacctgaggtga-3′	591 bp
BMP4 (NM_007554)	Forward, 5′-aaccgaatgctgatggtcgt-3′; reverse, 5′-acctcattctctgggatgct-3′	446 bp
Myogenin (NM_031189)	Forward, 5′-agcatcacggtggaggatat-3′; reverse, 5′-agaagaggatgctctctgct-3′	285 bp
MyoD1 (NM_010866)	Forward, 5′-tccaactgctctgatggcat-3′; reverse, 5′-tgctgctgcagtcgatctct-3′	370 bp
α-MHC (NM_010856)	Forward, 5′-tgctcgaggagatgcgagat-3′; reverse, 5′-tcttgagctctgagcactca-3′	540 bp
cTnT (NM_011619)	Forward, 5′-tacagactctgatcgaggct-3′; reverse, 5′-ttggtcttcattcaggtggt-3′	371 bp
Mef2C (NM_025282)	Forward, 5′-acagcaatcctgtcagcaca-3′; reverse, 5′-actgatggcatcgtgttctt-3′	340 bp
Axin2 (NM_015732)	Forward, 5′-tggacttctggtttgcttgt-3′; reverse, 5′-acgtccactcctcttcttca-3′	385 bp
Dkk1 (NM_010051)	Forward, 5′-tggcttgcaggatacagaaa-3′; reverse, 5′-acaggtaagtgccacactga-3′	302 bp
c-Myc (NM_010849)	Forward, 5′-agctgtttgaaggctggatt-3′; reverse, 5′-tctcctccaagtaactcggt-3′	387 bp
ANP (NM_008725)	Forward, 5′-aacctgctagaccacctgga-3′; reverse, 5′-aagctgcgtgacacaccaca-3′	420 bp
BNP (NM_008726)	Forward, 5′-aagacaccagtgcacaagct-3′; reverse, 5′-agccaggaggtcttcctaca-3′	462 bp
β-MHC (NM_080728)	Forward, 5′-tgaccagctgatcaagaaca-3′; reverse, 5′-agcttcttctgcagctgact-3′	599 bp

and *Xenopus*, whereas it enhances cardiogenesis in *Drosophila* and a mouse teratocarcinoma cell line.

In previous study, RGS19 inhibits $G\alpha_o$ subunit activation by the Wnt signal. Expression of RGS19 attenuates Dvl phosphorylation, β-catenin accumulation, and Wnt-responsive gene transcription and blocks Wnt-induced differentiation of mouse F9 teratocarcinoma cells by inactivation of $G\alpha_o$. However, the knockdown of RGS19 expression also suppresses the Wnt signal (16).

In the present study, we examined the potential mechanisms involved in attenuating Wnt signaling during cardiac muscle differentiation. Transgenic mice that overexpressed RGS19 were produced to elucidate the role of RGS19 mouse cardiac development. Cardiomyocyte differentiation *in vitro* and analysis of cardiac development and ventricle repolarization in mice were performed to examine the roles of RGS19.

EXPERIMENTAL PROCEDURES

Plasmid Construct—The murine RGS19 gene was amplified from mouse embryo RNA. An EcoRI, BamHI fragment containing the full length of the mouse RGS19 cDNA was cloned into the pEGFP-N1 vector driven by the CMV promoter. This expression cassette was prepared by digesting the recombinant vector with DraIII for transfection or microinjection. Plasmid DNA was purified using a midi-prep kit (Qiagen, Valencia, CA).

Cell Culture, Differentiation, and Transfection—Cells were grown on 10-cm dishes in α-modified essential medium (Invitrogen) supplemented with 10% fetal bovine serum (FBS) (Invitrogen), penicillin, and streptomycin. The subculture was a ratio of 1:10 every 2–3 days and freshly replaced every 3 days. For the Wnt3a treatment experiment, recombinant mouse Wnt3a proteins were purchased from R&D Systems (Minneapolis, MN). Cells (5.0×10^5) were seeded in a culture dish, and Wnt3a protein was added to the culture medium at a concentration of 100 ng/ml. After 24 h, cells were harvested for RNA extraction. To induce differentiation, cells were seeded in a 1:40 dilution with α-modified essential medium, 10% FBS, and 1% dimethyl sulfoxide into bacterial grade Petri dishes for 4 days, after which the aggregates were plated back gently onto tissue culture dishes in growth media. For each experiment, cardiomyocyte differentiation was verified in the control cultures as spontaneous beating, starting at 9∼10 days. Cells were transfected using Lipofectamine™ 2000 (Invitrogen), and a stable cell line was maintained in a medium containing 400 μg/ml geneticin (Invitrogen). A day before transfection, 5×10^5 of the P19 cells were plated in 2 ml of the medium/well. For each well, 5 μl of Lipofectamine reagent was mixed with 2 μg of the RGS19 vector in serum-free Opti-MEM® (Invitrogen) to allow the DNA-Lipofectamine reagent complexes to form. The complexes were added to each well and mixed by gently rocking the plate back and forth. After 12 h, the cells were incubated in a CO_2 incubator at 37 °C for 24 h in α-modified essential medium supplemented with 10% FBS. To establish stable P19 cell lines, cells were selected in a medium containing 800 μg/ml geneticin (Invitrogen).

RNA Extraction and RT-PCR—Total cellular RNA was extracted with TRIzol® Reagent (Invitrogen) and treated with DNase I, amplification grade, at a concentration of 1 unit/mg RNA. The first strand of cDNA synthesis was performed using an RT-PCR kit (Promega, Madison, WI) with 1 μg of total RNA. Reverse transcription was performed in the presence of an oligo(dT)-primer with avian myeloblastosis virus reverse transcriptase. The reaction was incubated at 70 °C for 10 min and then at 42 °C for 60 min. Following 42 °C incubation, avian myeloblastosis virus reverse transcriptase was denatured at 95 °C for 5 min and stored at −20 °C until use. Taq DNA polymerase (Takara Bio, Tokyo, Japan) was used to perform with 32 cycles of PCR (94 °C, 57–64 °C, and 72 °C; all for 30 s). The amount of first strand reaction added to the PCR was titrated for each set of primers (Table 1). Primers were as follows for GAPDH: forward 5′-AATGCATCCTGCACCACCAA-3′ and reverse 5′-GTAGCCATATTCATTGTCATA-3′ (cycling profile: 94 °C, 57 °C, and 72 °C all for 30 s and 28 cycles).

Western Blot—To detect β-catenin, phospho-β-catenin, phospho-AKT, RGS19 (Abcam, Cambridge, MA), AKT (Cell Signaling Technology), and P19 cells were stimulated with 100 ng/ml of Wnt3a for 24 h. Cells were washed twice with PBS, and cell lysates were prepared in a lysis buffer. As a loading control, whole-cell lysates were blotted with anti-β-actin antibody. In RGS19 TG mice, β-catenin, phospho-AKT (Abcam) and RGS19 were observed to regulate Wnt signaling. C57BL/6 mice were used as a control.

Immunocytochemistry—Cells were seeded onto glass coverslips and cultured with dimethyl sulfoxide for 12 or 15 days. Immunostaining for cardiac troponin T (cTnT), α-myosin heavy chain (α-MHC) was performed using fluorescein isothiocyanate-conjugated rabbit polyclonal antibody. Cells were fixed with 4% paraformaldehyde and permeabilized with 0.2% Triton X-100 for 5 min. To detect cTnT, cTnT antibody was used (Santa Cruz Biotechnology, Santa Cruz, CA) Also, α-MHC antibody was used (Abcam). Nuclei were counterstained with 4′,6-diamidino-2-phenylindole.

Generation and Screening of Transgenic Mice—A diagram illustrating the DNA cassette used to generate TG mice is shown below (see Fig. 4). The murine RGS19 gene was amplified from the mouse embryo RNA by PCR with two pairs of primers encompassing the open reading frame region. The forward primer had an EcoRI site, and the reverse primer has a BamHI site for cloning. The resulting PCR product was cloned into the pEGFP-N1 vector to generate the pRGS19 construct, which was verified by sequencing. Plasmid DNA for microinjection was purified using the plasmid midi-prep kit (Qiagen). The expression cassette was prepared by digesting the recombinant vector DNA with DraIII. RGS19 transgenic (RGS19 TG) mice were generated using a standard procedure (17). All mice were raised and kept under specific pathogen-free conditions. Genomic DNA was extracted from biopsied offspring tails, and the RGS19 transgene was identified by PCR followed by 1% agarose gel electrophoresis. The primers used were, forward 5′-CGTGTACGGTGGGAGGTCTA-3′ and reverse 5′-TGGTGCAGATGAACTTCAGG-3′. Amplification was carried out with a thermal cycler (Takara Bio) applying the following cycles: 94 °C for 30 s; 57 °C for 30 s; and 72 °C for 30 s for 30 cycles. The PCR products (970 bp) were identified by electrophoresis in 1% agarose gel.

Proliferation and Apoptosis Assay—We examined isolated hearts from postnatal and 12-week-old mice to check for cell proliferation and apoptosis. For cell proliferation, Ki67 antibody was used to detect the M phase in the cell cycle. A TUNEL assay was used to identify double-stranded DNA fragmentation, and characteristics of DNA degradation by apoptosis. The TUNEL assay was performed using an *in situ* apoptosis detection kit (Trevigen).

Hematoxylin and Eosin Staining—Cardiac muscle section were excised from normal and RGS19 TG mice hearts, fixed in 10% neutral buffered formalin for 1 day, and embedded in paraffin. The paraffin-embedded tissues were cut into 7-μm sections and mounted onto glass slides. The slides were deparaffinized and incubated in a graded series of alcohol before the staining procedure. The sectioned heart samples were stained with H&E and then examined under a light microscope.

Electrocardiogram Recording—Mice were anesthetized with avertin (10 g of tribromoethanol alcohol and 10 ml of tert-amyl alcohol stored at 4 °C as a stock solution). After complete induction of anesthesia, a three-lead electrocardiogram was taken. The leads were placed on the right foreleg, left foreleg, and left hind leg. The data were recorded for analysis using chart and scope software. To reduce tissue damage, the electrode was kept on the tissue for <1 or 2 min and repositioned at approximately the same location when subsequent recordings were necessary.

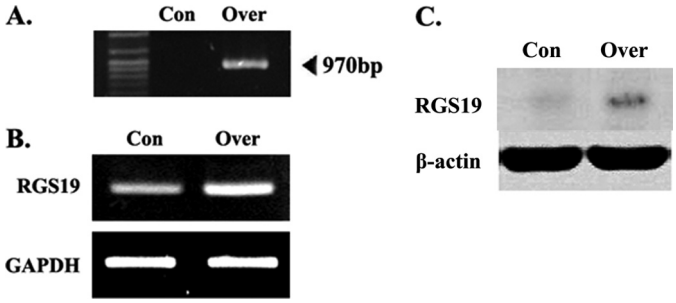

FIGURE 1. **Establishment of the RGS19 stable cell line.** *A*, two primers were used to detect fragments of contained ORFs by genomic PCR, as shown 970 bp. The forward primer was CGTGTACGGTGGGAGGTCTA, and reverse primer was TGGTGCAGATGAACTTCAGG. *B*, RGS19 was detected to quantitative expression by reverse-transcriptase PCR, as shown by a 373-bp DNA fragment. *C*, RGS19 was detected by Western blot. *Con*, control P19 cells; *Over*, RGS19-overexpressing cell line.

Statistical Analyses—Results are expressed as means ± S.E. from at least three independent experiments. Groups were compared by analysis of variance. Statistical significance was set at $p < 0.05$.

RESULTS

Stable Cell Line Establishment—After transfection into P19 cells, cells were treated with 800 μg/ml geneticin for selection. Colonies formed after 10 days and were transferred to 96-well plates. Among 150 colonies, five were sorted by genomic PCR (Fig. 1*A*). One colony was determined to have the highest expression levels and was therefore selected among those sorted. The mRNA expression level of RGS19 in RGS19 overexpression stable cells was highly expressed, compared with the control cell (Fig. 1*B*). Also, protein of RGS19 was increased (Fig. 1*C*).

Cardiac Muscle Differentiation in Vitro—A differentiation test on cardiomyocytes was performed using P19 cells. During the early stages of differentiation, expression changes in Brachyury T, a mesoderm early marker, were not visible. After 3 days of differentiation, Wnt3a expression in RGS19-overexpressing cells was not remarkably different than in control cells. However, measurements of GATA4 and BMP4, which are expressed during the middle stages of differentiation and are regulated by Wnt signaling, confirmed that expression was inhibited. Additionally, Pax3 expression was delayed *versus* the control. During the late stages of differentiation, MyoD1 and Myogenin expression were noticeably decreased (Fig. 2*A*). These results indicated that RGS19 overexpression inhibited cardiomyocyte differentiation. Expression patterns of differentiation-related genes were observed to determine how many cells are involved in heart function and which genes are related to contraction. Specifically, expression levels of the α-MHC and cTnT genes were quantified. We found that α-MHC and cTnT expression was inhibited noticeably (Fig. 2*D*). These results indicate that contraction was inhibited. For immunocytochemistry, expression of α-MHC and cTnT was detected and confirmed within 12 days, when differentiation was completed. RGS19-overexpressing cells showed decreased cTnT expression levels, compared with the

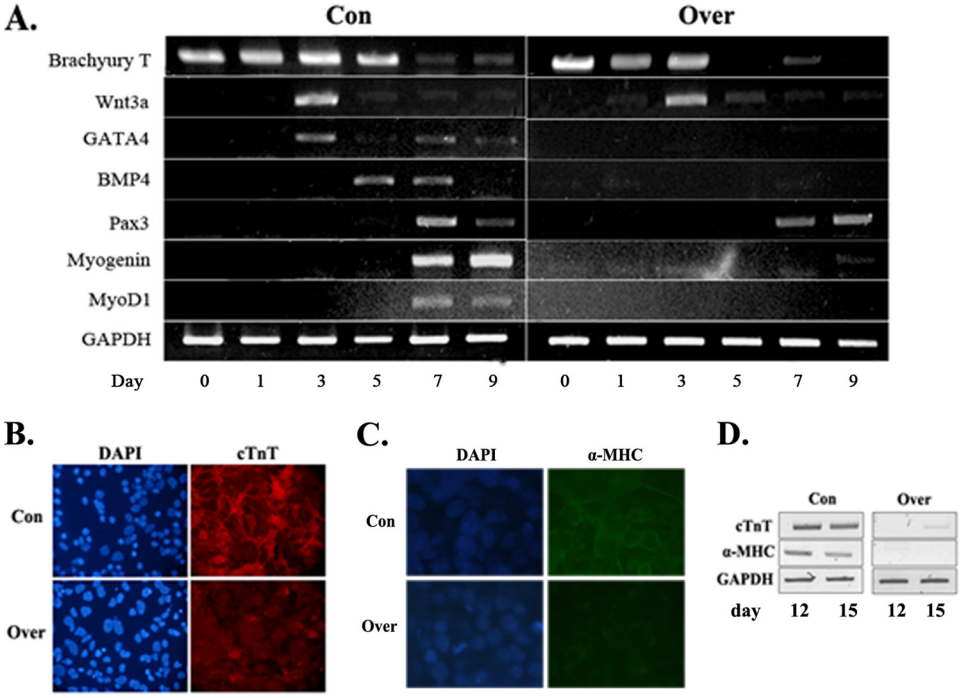

FIGURE 2. **Differentiation-related gene expression in cardiomyocyte differentiation.** *A*, this experiment used a P19 cell to differentiation with 1% dimethyl sulfoxide and culture for 9 days. A sample was prepared each day. *Con*, control P19 cells; *Over*, RGS19-overexpressing cell line. *Brachyury T*, mesoderm early maker; *GATA4*, cardiac muscle marker; *BMP4*, mesoderm marker; *Pax3*, muscle maker; *myogenin*, muscle maker; *MyoD1*, muscle maker. *B*, the protein expression of cTnT by immunocytochemistry in differentiated P19 cells at 12 days. *Red*, cTnT; *blue*, DAPI. *C*, the protein expression of α-MHC by immunocytochemistry in differentiated P19 cells at 12 days. *Green*, α-MHC; *Blue*, DAPI. *D*, expression of contraction-related genes by reverse-transcriptase PCR in P19 cells at 12 and 15 days. *Con*, control P19 cells, *Over*, RGS19-overexpressing cell line. The data are based on three independent experiments.

controls (Fig. 2*B*), and α-MHC expression levels decreased in RGS19-overexpressing cells, compared with the controls (Fig. 2*C*).

Regulation of Wnt-β-catenin Signal by RGS19 Overexpression—In the preceding experiment, RGS19 was confirmed to inhibit cardiomyocyte differentiation. We hypothesized that differentiation was blocked due to Wnt signal inhibition by RGS19, consistent with previous reports (16). When cells were treated with Wnt3a for 24 h, RGS19 should have inhibited Wnt signaling. Inactivation of β-catenin demonstrated that RGS19 overexpression induced phosphorylation of β-catenin Ser^{33}, 37 residues as compared with Wnt3a treatment of control cells. Moreover, phosphorylation of the AKT Thr^{308} residue, which is the active form, was reduced by RGS19 overexpression as compared with Wnt3a treatment of control cells (Fig. 3*A*). Expression levels of Wnt downstream signals, such as Dkk1, Axin, and c-Myc, which are regulated by Wnt, were examined. When treated with Wnt3a, Dkk1 and Axin expression levels decreased significantly com-

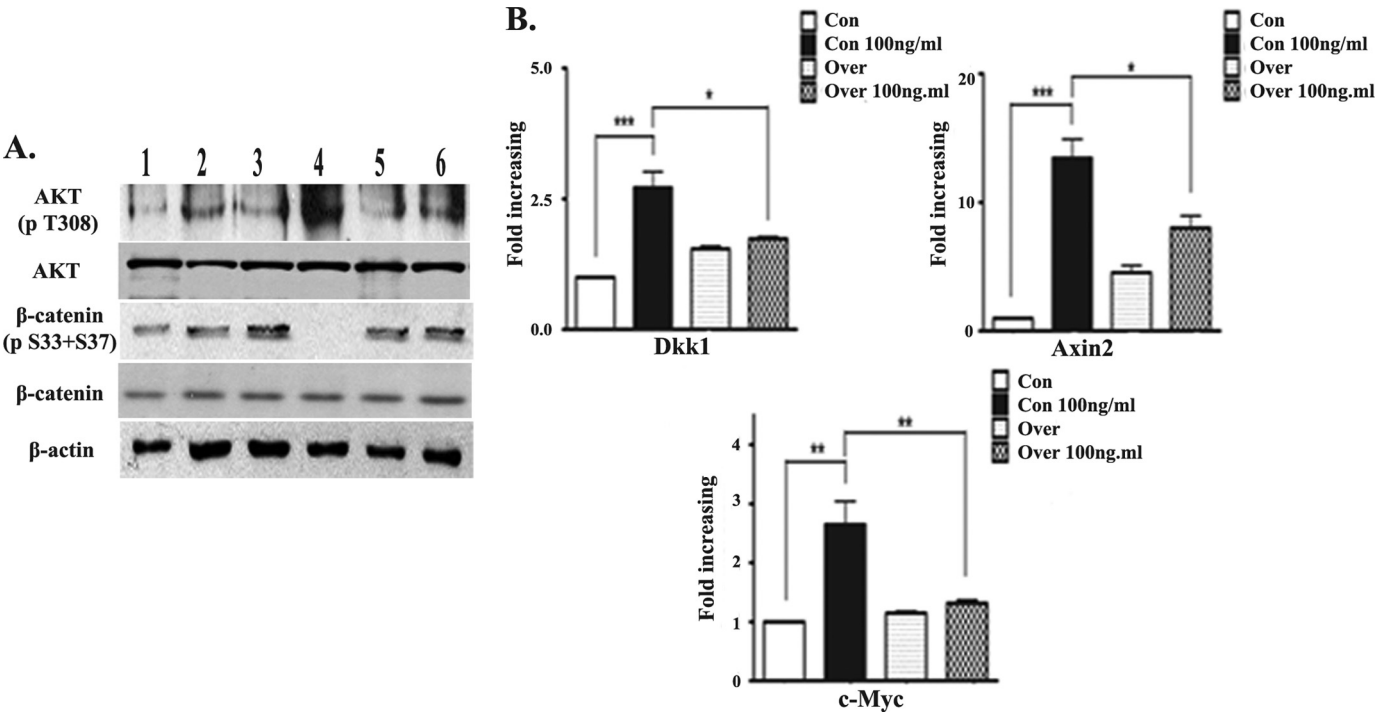

FIGURE 3. **Overexpression of RGS19 affects to the Wnt signal pathway.** *A*, modulation of RGS19 is examined by Western blot. *Lanes 1* and *4*, control P19; *lanes 2* and *5*, RGS19-overexpressing cells 1, *lanes 3* and *6*, RGS19-overexpressing cells 2; *lanes 1–3*, no treatment of Wnt3a; *lanes 4–6*, treatment of Wnt3a (*B*) mRNA expression of Dkk1, Axin, and c-Myc. Treated with 100 ng/ml Wnt3a for 24 h. *Con*, control P19 cells; *Over*, RGS19-overexpressing cell line. The data shown are the mean values of at least three separate experiments. *, $p < 0.05$; **, $p < 0.01$; ***, $p < 0.001$.

pared with the control (Fig. 3*B*; *, $p < 0.05$, ***, $p < 0.001$). Additionally, the expression of c-Myc, a transcription factor, also decreased significantly compared with the controls (Fig. 3*B*; **, $p < 0.01$). These data suggest that the Wnt signal was blocked during RGS19 inhibition of cardiomyocyte differentiation.

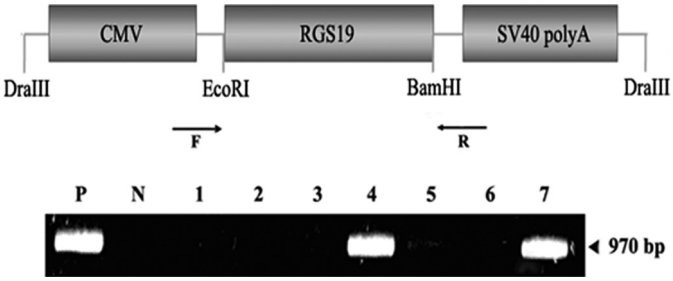

FIGURE 4. **RGS19 overexpression vector construct and generation.** The primers used for tail biopsy PCR are indicated as shown with 970-bp bands to indicate the RGS19 transgene. Two mice lines were confirmed as transgenic mice. *F*, forward primer; *R*, reverse primer. The same primers which were used for genomic PCR in the stable cell line were used to select TG mice.

Generation of Transgenic Mice—To generate RGS19-overexpressing transgenic (TG) mice, plasmids for transgene expression throughout the whole body were constructed. The CMV promoter was used to drive expression of the transgene (Fig. 4). The transgene construct was microinjected into mouse embryos. To identify transgenic mice, total genomic DNA was extracted from the biopsied tail of founder candidates, and PCR screening using specific primers was performed. As a result, two mouse lines were confirmed as transgenic (Fig. 4). When each founder mouse was mated with nontransgenic mice, all pups were able to produce offspring, and the transgene was inherited.

Cardiac Development during Embryonic Stages—RGS19 transgenic (RGS19 TG) mice gave birth to 5–8 offspring, compared with the wild-type mice, which produced 9–11 offspring. When the embryonic stage was examined between 13.5 and 16.5 days, it was noted that 10–12 embryos at 13.5 days survived. However, at 16.5 days, only 5–8 embryos were alive. Histological analysis of these RGS19 TG mice revealed abnormal ventricular development, including ventricular septal defect, a thin ventricular wall, and ventricular noncompaction (Fig. 5, *A–E*). Expression of numerous regulators of cardiogenesis, including BMP4 and Mef2C, were down-regulated in RGS19 TG mice (Fig. 5*F*; *, $p < 0.05$).

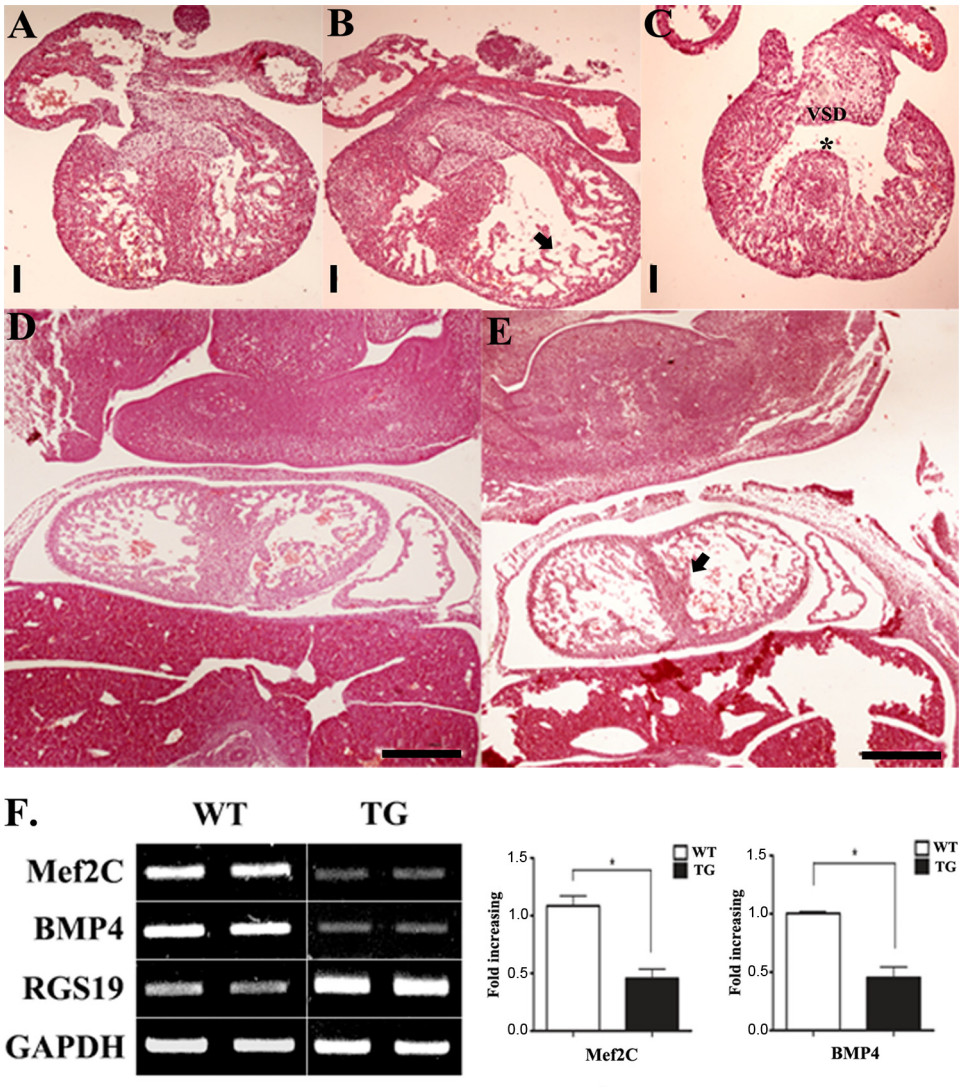

FIGURE 5. **Defects of cardiac development in RGS19-overexpressing TG mice at embryonic stages.** Heart isolated from 13.5 day mice was used for histological analyses stained with H&E. *A*, wild-type. *B* and *C*, RGS19 TG mice. *Arrows* indicate a thin vectricular wall. The *asterisk* indicates ventricle septal defect. *Scale bars*, 100 μm. Images of the whole embryo section are shown at 13.5 days by H&E staining. *D*, wild-type. *E*, RGS19 TG mice. *Arrow* indicates a thin vectricular wall. *Scale bars*, 500 μm. *F*, reverse transcriptase PCR of indicated genes from the heart of WT and TG embryo at 13.5 days. *, $p < 0.05$. *TG*, RGS19 TG mice.

Morphology and Cell Proliferation of Heart in Postnatal Mice—RGS19 TG mice were examined after birth. To determine whether RGS19 TG mice possessed affected cardiac morphology, hearts were stained with H&E during the early postnatal days and in 12-week-old female mice. Some littermates of the RGS19 TG mice died immediately after birth. Severe defects were observed (Fig. 6, *C* and *D*), compared with WT mice (Fig. 6*A*). Some littermates of the RGS19 TG mice survived with only mild defects, such as decreased ventricular wall thickness (Fig. 6*B*). Expressed Ki67 cells decreased in the RGS19 TG mice as compared with WT mice 0–2 days old. Thus, cell proliferation decreased, but apoptosis did not (data not shown).

Defect and Molecular Alteration of Heart in Transgenic Mice—In 12-week-old female mice, the ventricular wall was thinner in RGS19 TG mice compared with WT mice (Fig. 7*B*), as determined by trans-

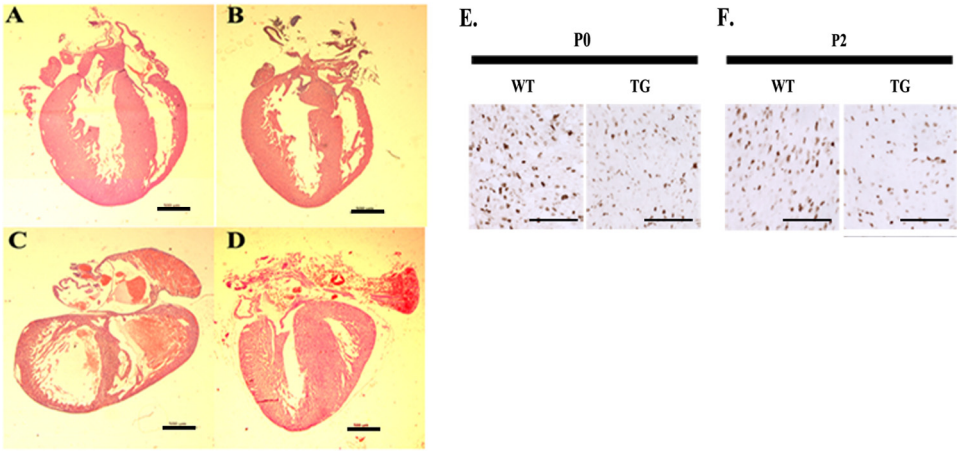

FIGURE 6. **Heart histology and cell proliferation of postnatal mice.** Histological analyses were stained with H&E postnatal mice. *A*, wild-type. *B*, long-lived RGS19 TG mice. *C* and *D*, short-lived RGS19 TG mice after birth. *E* and *F*, expressed cells of Ki67 examined for proliferation in postnatal 0 or 2 day mice as compared with WT mice. *A–D*, *scale bars*, 500 μm; *E* and *F*, *scale bars*, 50 μm.

verse section, compared with wild-type mice (Fig. 7*A*). Based on the cross-sectional area of the left ventricle, cardiomyocyte size decreased in the hearts of RGS19 TG mice (Fig. 7*D*). These conditioned mice appeared at a level of 23.5% (RGS19 TG offspring 8/34). Inactivation of β-catenin was induced in RGS19 TG mice in contrast to WT mice. Also, phosphorylation of AKT was elevated in RGS19 TG mice as compared with WT mice (Fig. 7*E*). The numbers of expressed cells of Ki67 increased in the RGS19 TG as compared with WT in 12-week-old mice. Thus, cell proliferation in-

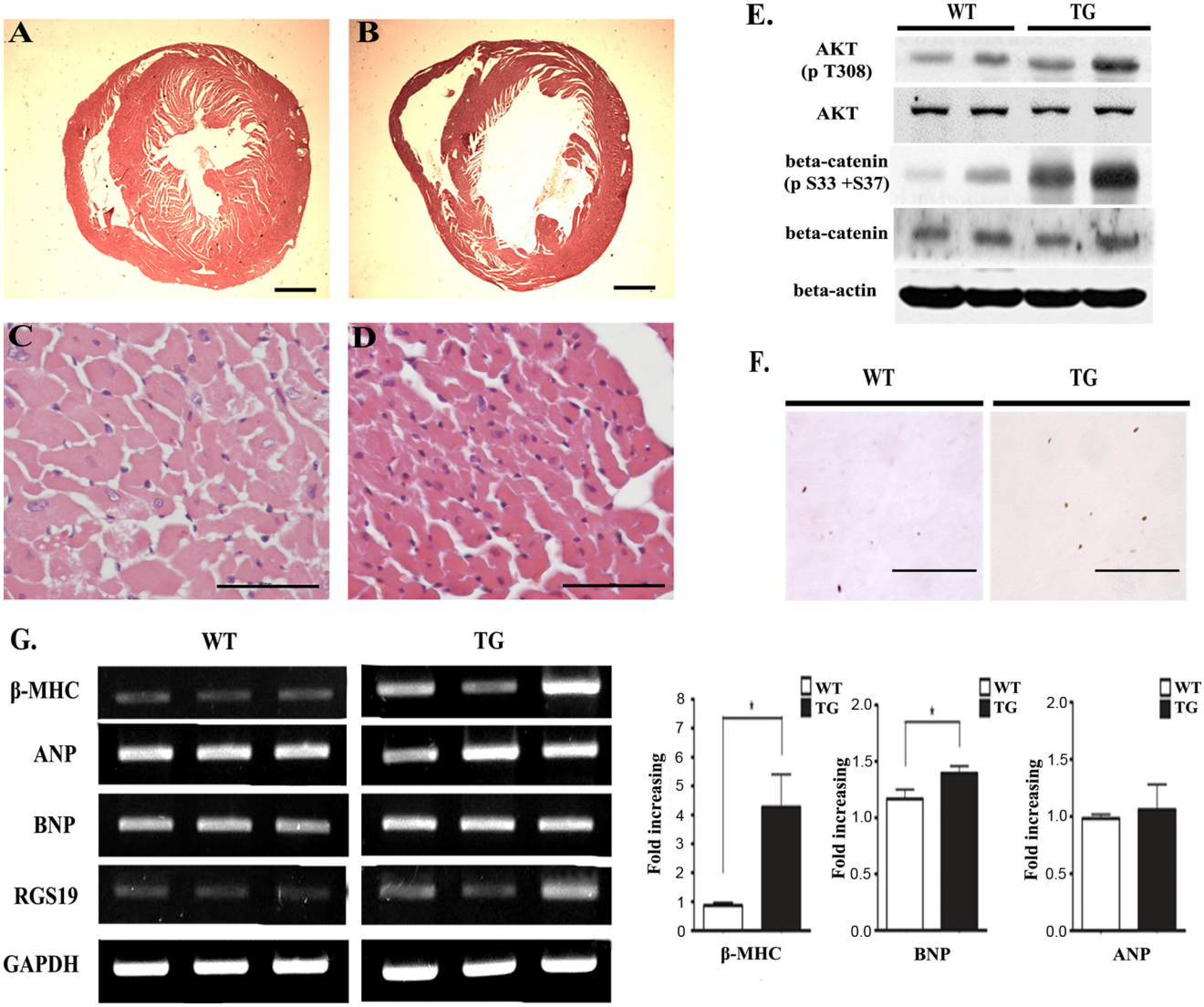

FIGURE 7. **Morphology and molecular alteration of heart are examined for detect effects of RGS19 in WT and TG mice at adult.** *A* and *C*, wild-type RGS19. *B* and *D*, TG mice. *Scale bars*, 700 μm. Representative heart transverse section of 12-week-old female mice. *E*, modulations of RGS19 are showed by phosphorylation of AKT, AKT, phosphorylation of β-catenin, and β-catenin *in vivo*. *F*, expression of Ki67 is performed for cell proliferation by immunohistochemistry in 12-week-old mice. *Scale bars*, 50 μm. *G*, reverse transcriptase PCR of indicated genes from the heart of WT and TG mice at 3 months. *, $p < 0.05$. *TG*, RGS19 TG mice.

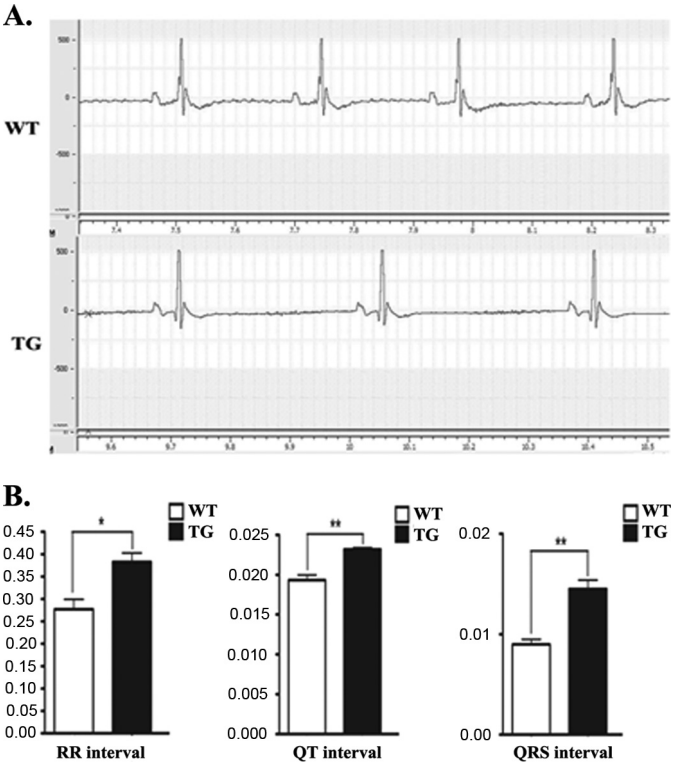

FIGURE 8. **Electrocardiogram analyses.** Shown is a representative cardiac repolarization by electrocardiography. *A*, an electrocardiogram of wild-type mice (*upper panel*) and RGS19 TG mice (*lower panel*). *B*, graph of electrocardiography parameter. *TG*, RGS19 TG mice. *, $p < 0.05$; **, $p < 0.01$.

creased (Fig. 7*F*), but not apoptosis (data not shown). mRNA levels of BNP and β-MHC genes, pathological markers of heart failure, were elevated significantly in RGS19 TG mice (Fig. 7*G*; *, $p < 0.05$), but that of atrial natriuretic peptide genes was not.

Electrocardiogram Analysis in Transgenic Mice—Electrocardiogram analysis was performed to examine heart function. In this experiment, three female mice were used. Electrocardiograms are shown separately (Fig. 8*A*). The RR, QT, and QRS intervals of transgenic female mice were increased, compared with wild-type female mice (Fig. 8*B*; *, $p < 0.05$; **, $p < 0.01$). These data showed that RGS19 affected heart function in TG mice.

DISCUSSION

This study demonstrates that the overexpression of RGS19 by P19 cells inhibited cardiomyocyte differentiation *in vitro*. Furthermore, the genes regulated by Wnt3a in an RGS19-overexpressing cell line decreased, compared with control cells. Without treatment with Wnt3a, the cell line overexpressing RGS19 showed increased expression of Dkk1 and Axin as compared with controls. Two factors are well known negative regulators in the canonical Wnt pathway (18, 19). These results suggest that the increase in Dkk1 and Axin by overexpression of RGS19 may inhibit the canonical Wnt pathway. Moreover, activation of AKT and β-catenin, well known positive factors, was inhibited. This regulation also blocked the canonical Wnt pathway and inhibited cardiomyocyte differentiation.

In the case of RGS19 TG mice, morphologic cardiac abnormalities (ventricle wall thinning and ventricle septal defects) were present in the embryo. Expression of genes during cardiogenesis was also down-regulated. Moreover, adult mice demonstrated ventricular wall thinning, alteration of cell proliferation, and abnormal ventricle repolarization. An inactivated form of β-catenin was induced.

As discussed earlier, the Wnt/β-catenin signal is important in cardiac development. In the most recent studies, gains and losses of β-catenin function have been analyzed in knock-out or knock-in mouse models. In gain of function models, abnormal phenotypes appear to have enlarged second heart field derivatives, due to enhanced proliferation of the second heart field (20), disrupted heart tube formation (21), a shortened right ventricle, and density of the outflow tract myocardium (22). In loss of function models, various abnormal phenotypes with defects in second heart field proliferation (20), the outflow tract, the right ventricle (22, 23), endocardial cushion formation (24), coronary artery formation (25), and multiple heart formation have been observed (26). In our results, RGS19 TG mice exhibited ventricular wall thinning and ventricular septal defects, finding similar to those observed in β-catenin deletion mice. Furthermore, β-catenin was reported recently to regulate cardiac hypertrophy (27, 28). Thus, RGS19 may affect cardiac hypertrophy in TG mice.

BMP4, a secretion factor involved in cardiac development, was blocked by RGS19 expression. In the present study, the loss of BMP4 expression resulted in cushion remodeling and ventricular septal defects (29). Our results showed that expression of BMP4 decreased during heart development, and the same cardiac development defects were detected in RGS19 TG mice. This suggests that RGS19 regulates the expression of BMP4 and that this regulation affects embryonic cardiac development.

In the differentiation method for this study *in vitro*, P19 cells generally differentiated into cardiomyocytes or skeletal muscle. We examined using methods differentiated into only cardiomyocyte, but not skeletal muscle (30). Activation of the Wnt/β-catenin signaling pathway is an early stage in cardiomyocyte differentiation of pluripotent P19 cells, as measured by Wnt3a. Wnt/β-catenin signals are essential for *in vitro* cardiomyocyte differentiation of mouse P19 cells, a teratocarcinoma-derived pluripotent cell line (15, 31). Inactivation of β-catenin demonstrated the same *in vivo* and *in vitro* expression, but activation of AKT resulted in different patterns environmental and regulatory factors vary between *in vivo* and *in vitro* models.

In our study, activation of AKT was induced in RGS19 TG mice in contrast to WT mice. In this case, activation of AKT may confirm a role of compensation in heart defects. For example, cardiac hypertrophy research shows that the AKT signal is activated (32, 33). Moreover, cardiomyocyte proliferation is detected in hypertrophy. Our results showed that cell proliferation increased when heart defects were detected in 12-week-old mice, suggesting that heart defects resulting from RGS19 overexpression may be compensated by activation of the AKT signal. Thus, our results showed that the activation of AKT was induced in RGS19 TG mice.

In RGS19 TG mice constructed using the CMV promoter, a previous study (44) demonstrated various levels of expression in different tissues. This study showed that RGS19 is expressed in the heart. In a subsequent study, because CMV promoter

activity and expression levels differ, we checked the expression levels of RGS19 in different cell types and organs and at different developmental stages.

In further studies, because the Wnt signal pathway regulates the development and function of various organ systems, we need to search for its effect on other organs. In previous studies, deletion of β-catenin led to changes in osteoblastogenesis and chondrogenesis (34, 35); impaired differentiation of neuromuscular junctions; abnormal midbrain, and cerebellum structures in the central nervous system (36, 37); abnormal lens morphology in the eye (38); impaired hematopoietic stem cell self-renewal (39); and defects in hepatoblast expansion and maturation in the liver (40). In addition to the systems mentioned, Wnt signaling plays a major role in many organs (41–43). Moreover, the effects of RGS19 down-regulation or knock-out need to be investigated in the Wnt signal. In summary, RGS19 negatively affects and plays an important role in cardiac development and function.

REFERENCES

1. De Vries, L., Zheng, B., Fischer, T., Elenko, E., and Farquhar, M. G. (2000) *Annu. Rev. Pharmacol. Toxicol.* **40,** 235–271
2. Ross, E. M., and Wilkie, T. M. (2000) *Annu. Rev. Biochem.* **69,** 795–827
3. Hollinger, S., and Hepler, J. R. (2002) *Pharmacol. Rev.* **54,** 527–559
4. De Vries, L., Mousli, M., Wurmser, A., and Farquhar, M. G. (1995) *Proc. Natl. Acad. Sci. U.S.A.* **92,** 11916–11920
5. Moon, R. T., Bowerman, B., Boutros, M., and Perrimon, N. (2002) *Science* **296,** 1644–1646
6. Kimelman, D. (2006) *Nat. Rev.* **7,** 360–372
7. Yamaguchi, T. P. (2001) *Curr. Biol.* **11,** R713–724
8. Liu, T., DeCostanzo, A. J., Liu, X., Wang, Hy, Hallagan, S., Moon, R. T., and Malbon, C. C. (2001) *Science* **292,** 1718–1722
9. Cabrera-Vera, T. M., Vanhauwe, J., Thomas, T. O., Medkova, M., Preininger, A., Mazzoni, M. R., and Hamm, H. E. (2003) *Endocr. Rev.* **24,** 765–781
10. Ikeda, S., Kishida, S., Yamamoto, H., Murai, H., Koyama, S., and Kikuchi, A. (1998) *EMBO J.* **17,** 1371–1384
11. Aberle, H., Bauer, A., Stappert, J., Kispert, A., and Kemler, R. (1997) *EMBO J.* **16,** 3797–3804
12. Tzahor, E., and Lassar, A. B. (2001) *Genes Dev.* **15,** 255–260
13. Schneider, V. A., and Mercola, M. (2001) *Genes Dev.* **15,** 304–315
14. Park, M., Wu, X., Golden, K., Axelrod, J. D., and Bodmer, R. (1996) *Dev. Biol.* **177,** 104–116
15. Nakamura, T., Sano, M., Songyang, Z., and Schneider, M. D. (2003) *Proc. Natl. Acad. Sci. U.S.A.* **100,** 5834–5839
16. Feigin, M. E., and Malbon, C. C. (2007) *J. Cell Sci.* **120,** 3404–3414
17. Hogan, B., Costantini, F., and Lacy, E. (1986) *Manipulating the Mouse Embryo,* Cold Spring Harbor Laboratory Press, New York
18. Jho, E. H., Zhang, T., Domon, C., Joo, C. K., Freund, J. N., and Costantini, F. (2002) *Mol. Cell. Biol.* **22,** 1172–1183
19. Korol, O., Gupta, R. W., and Mercola, M. (2008) *Dev. Biol.* **324,** 131–138
20. Klaus, A., Saga, Y., Taketo, M. M., Tzahor, E., and Birchmeier, W. (2007) *Proc. Natl. Acad. Sci. U.S.A.* **104,** 18531–18536
21. Cohen, E. D., Wang, Z., Lepore, J. J., Lu, M. M., Taketo, M. M., Epstein, D. J., and Morrisey, E. E. (2007) *J. Clin. Investig.* **117,** 1794–1804
22. Ai, D., Fu, X., Wang, J., Lu, M. F., Chen, L., Baldini, A., Klein, W. H., and Martin, J. F. (2007) *Proc. Natl. Acad. Sci. U.S.A.* **104,** 9319–9324
23. Kwon, C., Arnold, J., Hsiao, E. C., Taketo, M. M., Conklin, B. R., and Srivastava, D. (2007) *Proc. Natl. Acad. Sci. U.S.A.* **104,** 10894–10899
24. Liebner, S., Cattelino, A., Gallini, R., Rudini, N., Iurlaro, M., Piccolo, S., and Dejana, E. (2004) *J. Cell Biol.* **166,** 359–367
25. Zamora, M., Männer, J., and Ruiz-Lozano, P. (2007) *Proc. Natl. Acad. Sci. U.S.A.* **104,** 18109–18114
26. Lickert, H., Kutsch, S., Kanzler, B., Tamai, Y., Taketo, M. M., and Kemler, R. (2002) *Dev. Cell* **3,** 171–181
27. Qu, J., Zhou, J., Yi, X. P., Dong, B., Zheng, H., Miller, L. M., Wang, X., Schneider, M. D., and Li, F. (2007) *J. Mol. Cell Cardiol.* **43,** 319–326
28. Baurand, A., Zelarayan, L., Betney, R., Gehrke, C., Dunger, S., Noack, C., Busjahn, A., Huelsken, J., Taketo, M. M., Birchmeier, W., Dietz, R., and Bergmann, M. W. (2007) *Circ. Res.* **100,** 1353–1362
29. McCulley, D. J., Kang, J. O., Martin, J. F., and Black, B. L. (2008) *Dev. Dyn.* **237,** 3200–3209
30. Skerjanc, I. S. (1999) *Trends Cardiovasc. Med.* **9,** 139–143
31. Naito, A. T., Akazawa, H., Takano, H., Minamino, T., Nagai, T., Aburatani, H., and Komuro, I. (2005) *Circ. Res.* **97,** 144–151
32. Braz, J. C., Gill, R. M., Corbly, A. K., Jones, B. D., Jin, N., Vlahos, C. J., Wu, Q., and Shen, W. (2009) *Eur. J. Heart Fail* **11,** 739–748
33. Howes, A. L., Miyamoto, S., Adams, J. W., Woodcock, E. A., and Brown, J. H. (2006) *J. Mol. Cell Cardiol.* **40,** 597–604
34. Day, T. F., Guo, X., Garrett-Beal, L., and Yang, Y. (2005) *Dev. Cell* **8,** 739–750
35. Hill, T. P., Später, D., Taketo, M. M., Birchmeier, W., and Hartmann, C. (2005) *Dev. Cell* **8,** 727–738
36. Schüller, U., and Rowitch, D. H. (2007) *Brain Res.* **1140,** 161–169
37. Li, X. M., Dong, X. P., Luo, S. W., Zhang, B., Lee, D. H., Ting, A. K., Neiswender, H., Kim, C. H., Carpenter-Hyland, E., Gao, T. M., Xiong, W. C., and Mei, L. (2008) *Nat. Neurosci.* **11,** 262–268
38. Smith, A. N., Miller, L. A., Song, N., Taketo, M. M., and Lang, R. A. (2005) *Dev. Biol.* **285,** 477–489
39. Scheller, M., Huelsken, J., Rosenbauer, F., Taketo, M. M., Birchmeier, W., Tenen, D. G., and Leutz, A. (2006) *Nat. Immunol.* **7,** 1037–1047
40. Tan, X., Yuan, Y., Zeng, G., Apte, U., Thompson, M. D., Cieply, B., Stolz, D. B., Michalopoulos, G. K., Kaestner, K. H., and Monga, S. P. (2008) *Hepatology* **47,** 1667–1679
41. Liu, F., Thirumangalathu, S., Gallant, N. M., Yang, S. H., Stoick-Cooper, C. L., Reddy, S. T., Andl, T., Taketo, M. M., Dlugosz, A. A., Moon, R. T., Barlow, L. A., and Millar, S. E. (2007) *Nat. Genet.* **39,** 106–112
42. Rulifson, I. C., Karnik, S. K., Heiser, P. W., ten Berge, D., Chen, H., Gu, X., Taketo, M. M., Nusse, R., Hebrok, M., and Kim, S. K. (2007) *Proc. Natl. Acad. Sci. U.S.A.* **104,** 6247–6252
43. Malanchi, I., Peinado, H., Kassen, D., Hussenet, T., Metzger, D., Chambon, P., Huber, M., Hohl, D., Cano, A., Birchmeier, W., and Huelsken, J. (2008) *Nature* **452,** 650–653
44. Schmidt, E. V., Christoph, G., Zeller, R., and Leder, P. (1990) *Mol. Cell. Biol.* **10,** 4406–4411